Nanocomposites of poly(ε-caprolactone) doped with titanium species

A. V. Machado - S. Amorim - G. Botelho I.
C. Neves - A. M. Fonseca

Abstract

Organic-inorganic hybrid nanocomposites were prepared via in situ sol-gel process. The organic phase is a biodegradable polymer, poly(ε-caprolactone) (PCL), while the tetrabutyl titanate ($\mathrm{TBT, Ti(OBu)_4}$) was used as inorganic precursor. Synthesis parameters like acidity medium and precursor amount were investigated in order to assess their influence on hybrid properties. The obtained nanocomposites were characterised by thermal analysis, spectroscopic techniques, transmission electronic microscopy (TEM) and X-ray diffraction to gather information on the structure of the nanocomposites. Mechanical properties and biodegradability were also evaluated. A reaction mechanism based on Fourier transform infrared spectroscopy and NMR results was proposed using methyl acetate as model compound. TEM micrographs of the nanocomposites show a fine good nanoparticles dispersion. Acidic conditions and 10wt% of precursor lead to a nanocomposite with higher mechanical properties and biodegradability than PCL.

Introduction

Poly(ε-caprolactone) (PCL) is a biocompatible, biodegradable and permeable biopolymer with widespread use in a wide range of applications including textile, medical and packaging industries. However, it has low thermal stability,

low melting point and poor mechanical properties, which restrict its use in some applications. Thus, in order to enhance these properties, it is possible to combine organic and inorganic components to create novel materials [1]. These new materials combine the properties of the organic material, such as flexibility, toughness and processability, and of the inorganic, which gives thermal stability, durability and enhances mechanical properties [2]. If one of the phases has particles smaller than 100 nm , the material is called nanocomposite.

Inorganic precursors are usually metal alkoxides, $\mathrm{M[OC_nH_{2n^-+1}]}$ where $\mathrm{M = Si, Sn, Ti, Zr, Al}$ etc. The most common, used to develop hybrid organic-inorganic nanocomposites, is the silicon alkoxide [3, 4]. However, titanium (Ti) precursors have received great interest and have been target in recent studies, due to the possibility of obtaining higher refractive index materials [5, 6]. To prepare these nanocomposites, sol-gel process is one of the most valid methods since it enables to control and manipulate its structure. This type of synthesis involves two steps, hydrolysis and condensation of metal alkoxide. However,

when the synthesis involves Ti precursor, the process is not that simple. Since Ti is a transition metal, it is very difficult to control the process due to the high reactivity of this group of metals, especially with d^0 orbital. When the alkoxide ligand has high electronegativity, it will induce the metal to become more electropositive and consequently more susceptible to nucleophilic attack [7]. Moreover, the reactivity depends not only on the electrophilicity of the metal, but also on their degree of unsaturation. Ti transition metal has higher degree of insaturation, making them coordinatively unsaturated and may expand its coordination state through nucleophilic reaction [8].

Previous studies [7, 9] indicated that the incorporation of large amounts of inorganic phase into polymer matrix by in situ sol-gel process leads to an increase of the melting point and a decrease of the crystallinity of the hybrid polymer.

Thus, the aim of this work is the synthesis and characterisation of organic-inorganic hybrid nanocomposites based on PCL using tetrabutyl titanate ($\mathrm{TBT, Ti(OBu)_4}$) as inorganic precursor. The study started with the synthesis of the nanocomposite using a model compound of PCL, methyl acetate, to understand the mechanism and the structure of the final hybrid. Different synthesis conditions (acid concentration and precursor amount) were investigated to assess their influence on the final nanocomposite properties. The prepared nanocomposites were characterised by thermal analysis (thermogravimetry analysis [TGA] and differential scanning calorimetry [DSC]), X-ray diffraction (XRD), X-ray photoelectron spectroscopy (XPS), transmission electronic microscopy (TEM) and Fourier transform infrared spectroscopy (FTIR) to gather information on the structure, morphology and properties of the new materials. Biodegradability was also evaluated.

Experimental

Materials

TBT (98 %) ($\mathrm{Ti(OBu)_4}$, Vertec), chloroform ($\mathrm{CHCl_3}$, LABSCAN), concentrated hydrochloric acid (37%) (HCl , Aldrich) and methyl acetate (99%) ($\mathrm{CH_3COOCH_3}$, Panreac) were purchased as analytical grade reagents and used without further purification. PCL in granulated form (Capa $\mathrm{FB100, MFI = 0.4\ g/10\ min}$ at $\mathrm{190°C/2.16\ kg}$) was kindly supplied by Solvay.

Hybrid nanocomposites synthesis

Different hybrid nanocomposites were prepared in order to study the influence of the inorganic precursor amount and the effect of the acid. Therefore, organic and inorganic phases, PCL and TBT, respectively, were dissolved in different ratios. In the presence of HCl(0.07HCl/TBT, v/v), the amount of TBT used was 1, 5 or 10 (PCL/ TBT = 99/1,95/5 and 90/10w/w). The nomenclature of the nanocomposites was denoted PCL/TBT- X, where X is the TBT amount in weight percentage (wt%). The same amounts of TBT in the absence of HCl were used.

An example of the procedure used for the synthesis is: 1 mL of TBT was added to 2 mL of $\mathrm{CHCl_3}$, then 0.070 mL de HCl was added under vigorous stirring at room temperature

(solution 1). One gram of PCL was dissolved in 4 mL of $CHCl_3$, after complete dissolution of the polymer (solution 2) and added to solution 1 under vigorous stirring.

The homogeneous solution obtained was cast in a Teflon film and covered with a glass in order to slow the sol-gel process rate. After 24 h at room temperature, the film was dried in an oven at $85°C$ during 2 h .

The same experimental conditions were applied to prepare the hybrid with the model compound, methyl acetate (CH_3COOCH_3). More specifically, 1 mL of methyl acetate (12.7 mmol) and 1 mL of TBT (2.9 mmol) in the presence of acid and chloroform solution were used.

Characterisation techniques

FTIR spectra the samples were measured using a FTLA 2000 spectrometer, in a range between 4000 and 500 cm^{-1} using 10 scans and a nominal resolution of 4 cm^{-1}. While PCL and PCL nanocomposites the samples were analysed as films, KBr pellets were used for the model compound samples. ^{1}H and ^{13}C NMR spectra were obtained with 400 MHz in a Bruker Avance III+ 400, using as internal references the residual solvents. The samples were prepared using deuterated chloroform.

XPS analysis of the samples was performed using a Thermo Scientific K-Alpha ESCA instrument equipped with aluminium Ka1.2 monochromatized radiation at 1486.6 eV X-ray source. Due the non-conductor nature of samples it was necessary to use an electron flood gun to minimise surface charging. Surface charge neutralisation was performed using both low energy flood (electrons in the range $0 - 14eV$) and Argon ions gun. The XPS measurements were carried out using monochromatic Al-K radiation ($h = 1486.6eV$). Photoelectrons were collected from a take off angle of $90°$ relative to the sample surface. The measurement was done in a constant analyser energy mode with 100 eV pass energy for survey spectra and 20 eV pass energy for high resolution spectra. Charge referencing was done by setting the lower binding energy (BE) C 1s photopeak at 285.0 eV C 1s hydrocarbon peak. Surface elemental composition was determined using the standard Scofield photoemission cross sections.

Phase analysis was performed by XRD using a Philips PW1710 diffractometer. Scans were taken at room temperature in a 2θ range between $4°$ and $80°$, using $CuK\alpha$ radiation.

Samples of 70 nm thickness were cut using a diamond knife, in a Leica ultramicrotome at $-60°C$. The cut sections were transferred onto copper grids and then analysed without stain in a Philips CM120 TEM.

Thermal behaviour of the pure PCL, inorganic precursor and the nanocomposites were investigated by TGA and DSC. The thermogravimetric studies were performed using a TA Q500 thermobalance at a heating rate of $10\,°C min^{-1}$ from 30 to $600\,°C$, under argon atmosphere. DSC measurements were performed under argon atmosphere between 25 and $100°C$ at a heating rate of $10°C min^{-1}$ using a Mettler DSC 821e. The melting temperature (T_m) and crystallinity degree (X_c) were determined. While T_m was calculated by the computer software, X_c was determined by Eq. 1:

$X_c = \frac{\Delta H_f}{\Delta H_f^0}$,
where ΔH_f is the apparent melting enthalpy (indicated in DSC thermograms as melting enthalpy per gram) and ΔH_f^0 is the melting enthalpy per gram of the component in its completely crystalline state (139.5 J/g).

The mechanical properties of PCL and nanocomposites were characterised using stress-strain experiments in a ZWICK equipment. The tensile experiments were carried out with a deformation rate of 5.0 mm/min at room temperature and relative humidity of 50%. The tests were performed on 2.5 cm × 0.8 cm rectangular samples in a longitudinal direction. At least six specimens of each sample were tested. The thickness of every specimen was measured with a pachymeter Mitutoyo with an accuracy of 0.025 mm .

Biodegradation was assessed in aqueous environment under aerobic conditions according to the standard ISO 14851:1999, which specify a method for the determination of biochemical oxygen demand (BOD) in a closed respirometer. The complete procedure is described in Moura et al. [10].

Results and discussion

Synthesis parameters like acidity and inorganic precursor amount were studied in order to assess their influence on the nanocomposite properties. All sol-gel reactions were performed with chloroform, which does not coordinate with the transition metal.

A preliminary study was carried out using a PCL model compound, methyl acetate (CH_3COOCH_3), and the same inorganic precursor in order to find out the best conditions for nanocomposites synthesis and to better understand the reaction mechanism.

Synthesis of an organic-inorganic material based on the model compound

The hybrid was synthesized by sol-gel process using 90/10 (w/w), methyl acetate/TBT. Figure 1 shows the FTIR spectra of the inorganic precursor, methyl acetate and the prepared material.

The spectroscopic bands observed in the inorganic precursor and prepared hybrid, in the range of 31003700 cm^{-1}, are attributed to the stretching vibration of the

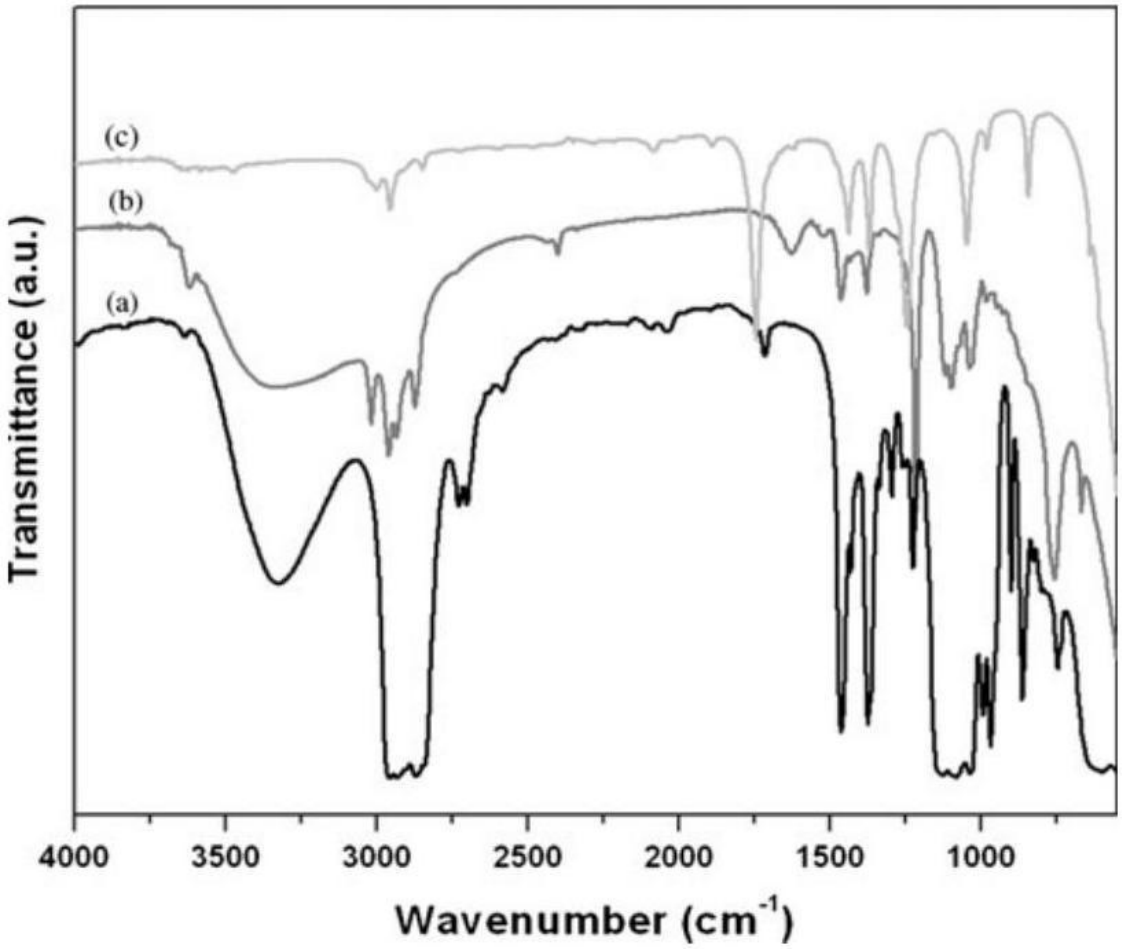

Fig. 1 FTIR spectra of the $(a)\mathrm{Ti(OBu)_4}$, (b) the prepared material and (c) methyl acetate

hydroxyl groups (Ti-OH), which is a product of the hydrolysis reactions [9,11]. The two small bands between 2000 and 2100 $\mathrm{cm^{-1}}$ are due to $\mathrm{C-H}$ stretching vibration of butoxide groups from the inorganic precursor. The bands in the region of $1000-1500\ \mathrm{cm^{-1}}$ are attributed to the deformation of alkyl chain of the precursor. A significant decrease of these bands can be noticed in the prepared hybrid indicating that hydrolysis of the inorganic precursor occurred. The deformation band typical of $\mathrm{Ti-OH}$ of the hybrid was shifted to $1634\ \mathrm{cm^{-1}}$ relatively to the one in the inorganic precursor [9]. The sharp band at $1750\ \mathrm{cm^{-1}}$ attributed to the carbonyl group presented in methyl acetate (Fig. 1c) is not presented in the hybrid and a new band at $1535\ \mathrm{cm^{-1}}$ can be observed. The latter was assigned by Mazzocchetti et al. [9] to carbonyl groups of the ester chain interacting with Ti via oxygen atom to fulfil metal electron deficiency. The obtained FTIR data indicate that the Ti has a different environment in the prepared material.

The $^{1}\mathrm{H}$ and $^{13}\mathrm{C}$ NMR spectroscopic analyses of the prepared hybrid, inorganic precursor and model compound in $\mathrm{CDCl_3}$ are presented in Table 1.

NMR spectroscopic data show one significant difference among the three spectra. The hybrid spectrum does not present any signal of the methyl group of the ester at $\delta =$ 3.20ppm.

Based on the FTIR and NMR data, it is possible to propose the reaction mechanism depicted in Scheme 1. This reaction is promoted in an acid medium, leading to the formation of the hydroxyl group, which reacts with methyl acetate to form titanium carboxylate. These reactions, involving carboxylates and Ti atoms have already been reported in the literature [12-15].

Table 1 ^{1}H and ^{13}C NMR data of inorganic precursor, metal acetate and hybrid material

	NMR δ (ppm)											
	$-Ti-OCH_2CH_2CH_2CH_3$								CCH_3		$COCH_3$	
	C_1		C_2		C_3		C_4					
	^{1}H	^{13}C	^{1}H	^{13}C	^{1}H	^{13}C	^{1}H	^{13}C	^{1}H	^{13}C	^{1}H	^{13}C
Ti(OBu)$_4$	4.30	74.28	1.61	35.58	1.35	19.09	0.92	13.94	-	-	-	-
CH_3CO_2(	-	-	-	-	-	-	-	-	1.58	19.11	3.20	50.16
Hybrid	4.00-4.04	64.57	1.49-1.63	31.68	1.24-1.42	18.81	0.83-0.93	13.94	1.49-1.63	19.01	-	-

Scheme 1 Reaction mechanism of Ti precursor with model compound

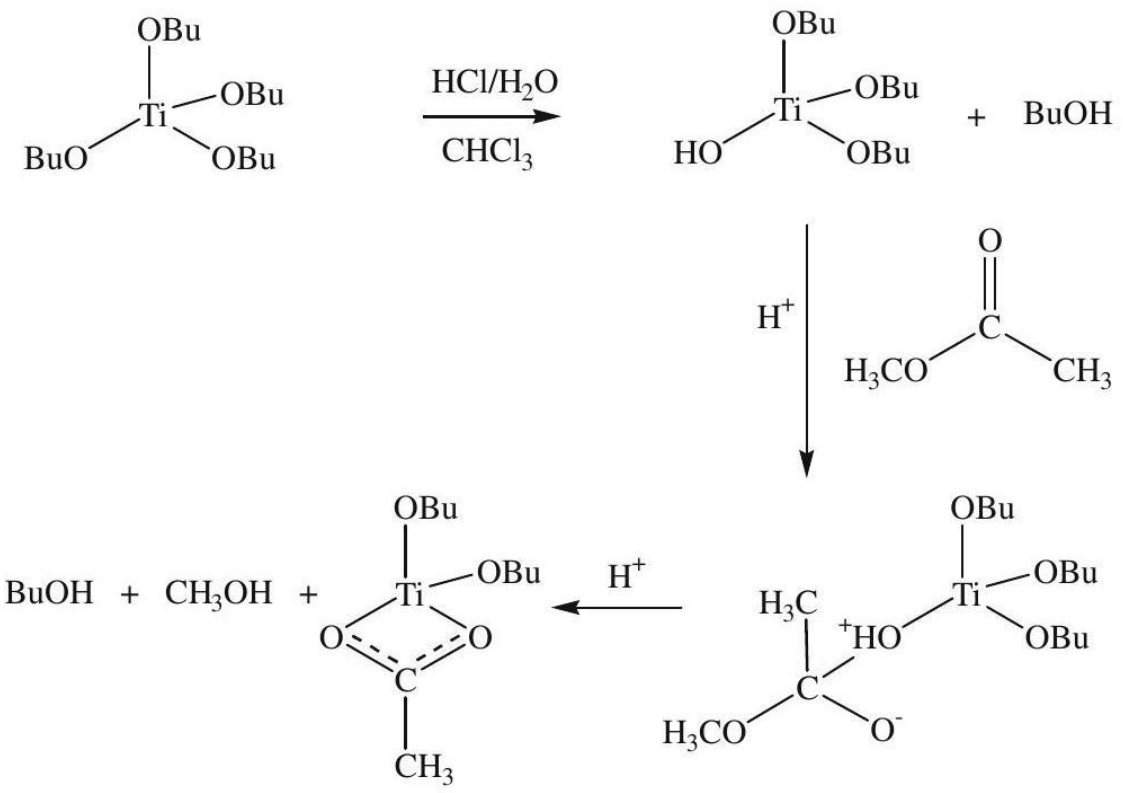

Synthesis of nanocomposites based on PCL

Effect of acid addition

Using the same experimental conditions that were used for the model compound, the organic-inorganic hybrid based on PCL was prepared. The acidity effect was investigated using the same synthesis procedure with and without hydrochloric acid. The composition was kept constant, being 90/10 (w/w) PCL/TBT. The FTIR spectra of PCL and synthesized nanocomposites are presented in Fig. 2.

FTIR spectra recorded for both nanocomposites are significantly different. FTIR spectrum of the hybrid prepared without acid has a new shoulder band centred at 1535 cm^{-1}. This band is typical from Ti-O-Ti network due to the condensation reaction [14]. Therefore, it seems that the interaction between PCL matrix and the titania network is mainly established by hydrogen bonds [7]. In the case of FTIR spectrum of the nanocomposite prepared with acid, the $Ti-OH$ groups are observed in the region $3100-3450$ cm^{-1}. The proton cation is expected to accelerate hydrolysis reaction, providing longer life to titanium hydroxide groups before condensation. TiO_2 formation is disfavoured and the probability of reaction between the polymer chains and

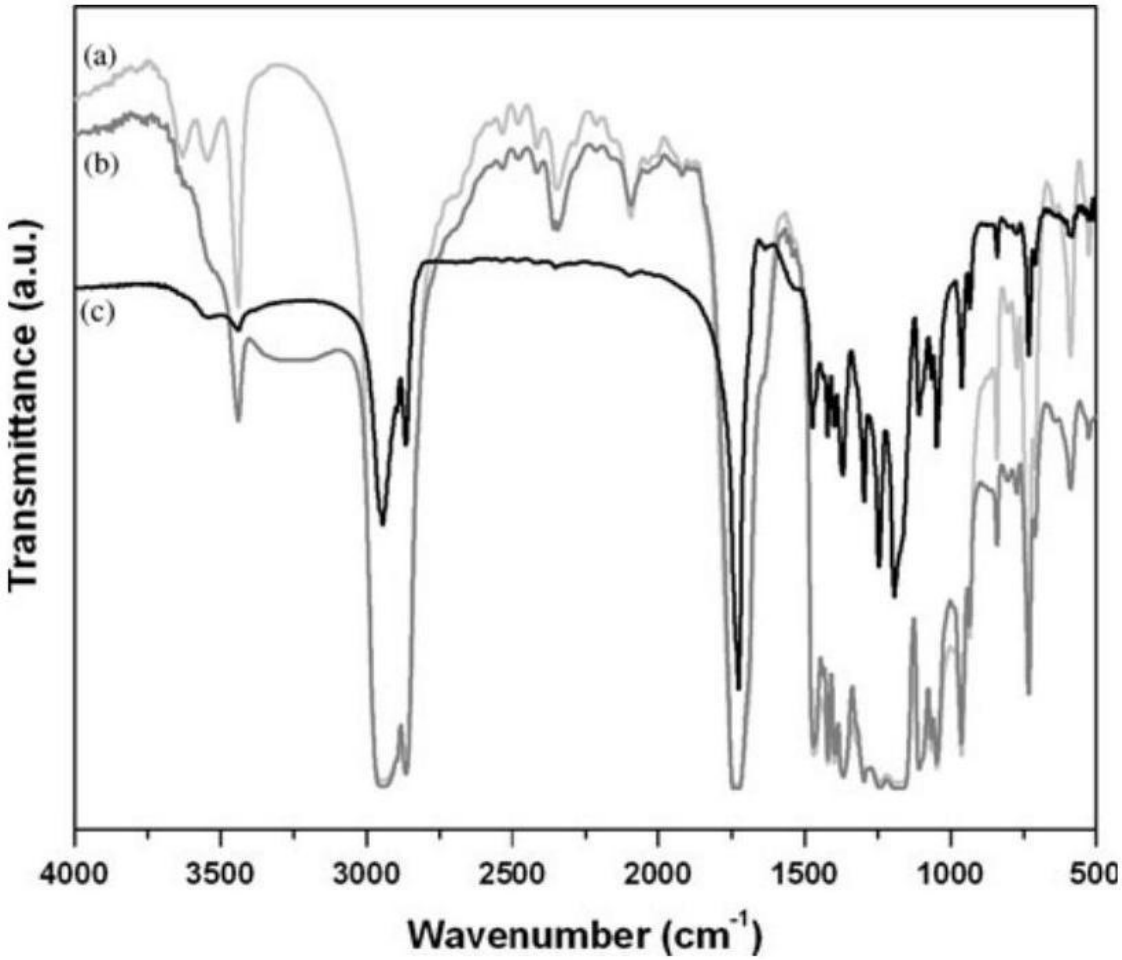

Fig. 2 FTIR spectra of (a) PCL, (b) PCL/TBT-10 with acid and (c) PCL/TBT-10 without acid

titanium hydroxide increases [9]. The acidity also influences the polymer reactivity, in fact transesterification is favoured in the presence of H^+that catalyses the interactions between carboxylic moiety and Ti atoms.

The XRD diffractograms of pure PCL and nanocomposites obtained with 10wt% of TBT with and without acid HCl are presented in Fig. 3.

The strong and sharp crystalline peaks at 21.2° and 23.7° are attributed to the (110) and (200) crystallographic planes of PCL crystal, respectively [7]. In both hybrids patterns, while the Miller indices of PCL did not change, the intensity of the diffraction peaks decreased significantly. PCL peaks can be observed in both hybrids at 2θ, 29.8°, 40.5° and 43.5°. The XRD diffraction patterns recorded for both hybrids are significantly different. The pattern of PCL/ TBT-10 without acid (Fig. 3b) reveals new peaks at 20, 36°, 38.3°, 48.3° and 52.6°, which are attributed to Ti in the anatase phase [16].

XPS has been used to identify the nature of chemical bonds between Ti , oxygen and carbon atoms in the nanocomposites [11, 17-19]. This technique can give information on the hydrolysis-condensation reaction extends with Ti precursor during the synthesis. The nanocomposites prepared with and without acid were analysed and Fig. 4 shows the survey of the hybrid PCL/TBT-10 with acid, as an example.

The spectrum shows the presence, at the sample surface, of carbon (C 1s photoelectron peak centred at 285.0 eV), Ti (Ti 2 p peak centred at 459.0 eV), oxygen (O 1 s peak centred at 533.0 eV) and silicon (Si 2 p peak centred at 103.0 eV). Silicon is attributed to a polydimethylsiloxane contamination that also contributes to the O 1 s peak [9]. Both samples show an intense asymmetric band at 285.0 eV in C 1s high resolution spectra that can be deconvoluted into three individual bands, which can be associated with different carbon species. These species are assigned to aliphatic carbons ($C-C, C-H; 285.0eV$), carbon atoms covalently bonded by a single bond to oxygen atoms ($C-O$; around 286.4 eV) and carbon atom of the carboxylate group ($C=O; 289.0eV$), which are characteristic of PCL chain. The O 1s high resolution spectrum shows an asymmetric band centred at 539.0 eV , which can

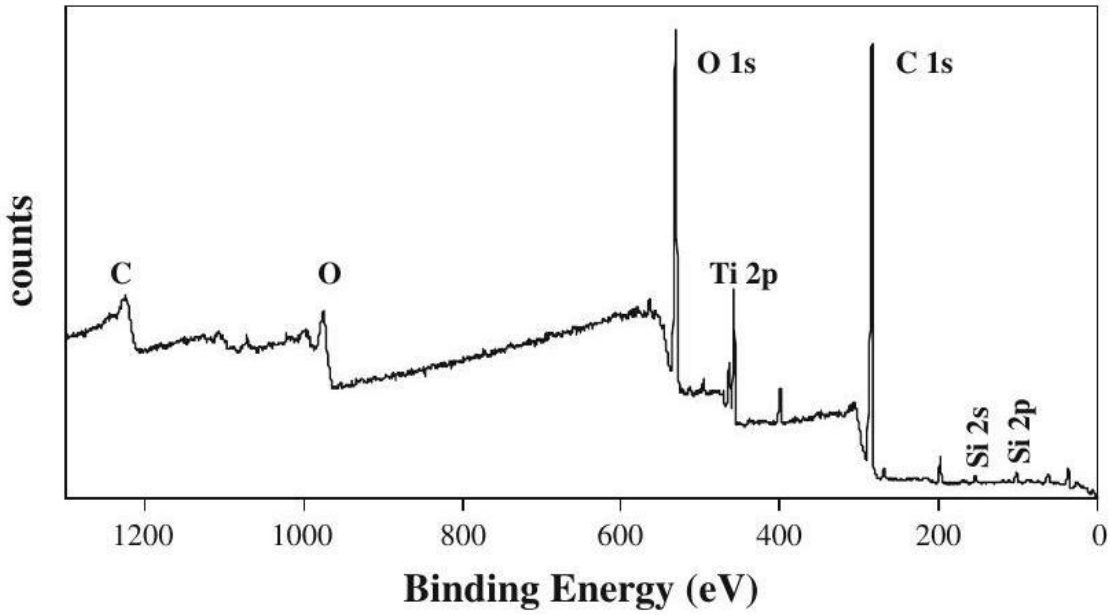

Fig. 4 Survey spectrum of PCL/TBT-10 with acid

also be deconvoluted into three individual bands that can be associated with different oxygen species, oxygen atoms bound to Ti in TiO_2, oxygen atoms covalently bonded by a single bond to carbon atoms from ester and oxygen atoms in carboxylate group ($O=C-O$; 533.5 eV) from PCL chain.

For both samples, the BE of the Ti species presents two photoelectronic peaks (Ti 2p) in the Ti 2p1/2 and Ti 2p p3/2 regions. The Ti $2p_{3/2}$ peak is centred at $458.7-459.0eV$, and the Ti $2p_{1/2}$ peak is found at $464.4-464.6eV$, with a spin energy separation of $5.7-5.6eV$. This is characteristic of the oxidation state Ti^{4+}, in good agreement with literature data [20-22]. In particular, the peak position of Ti^{4+} is significantly influenced by its coordination environment, and the Ti $2p_{3/2}$ peak of the octahedral coordinated Ti^{4+} generally locates at lower BE (about $457.8-458.3eV$), while that of tetrahedral coordinated Ti^{4+} at higher BE (about $458.5-463.4eV$) [20, 21, 23]. Tetrahedron and octahedral environments can be assigned to non-condensed and fully condensed titanium alkoxides, respectively. The observed BE Ti $2p_{3/2}$ values in the samples are different. For the nanocomposites prepared without acid, the values approach to a tetrahedral coordination. In acid medium, the values are close to those observed for the Ti in an

octahedral environment with the presence of different Ti species (TiO_2, $Ti-OH$, $Ti-O-C$), in agreement with FTIR data.

Fig. 3 Wide (I) and partial (II) XRD diffraction patterns of: (a) PCL, (b) PCL/TBT-10 without acid and (c) PCL/TBT10 with acid. The XRD peaks of the anatase phase were labelled with Miller indices

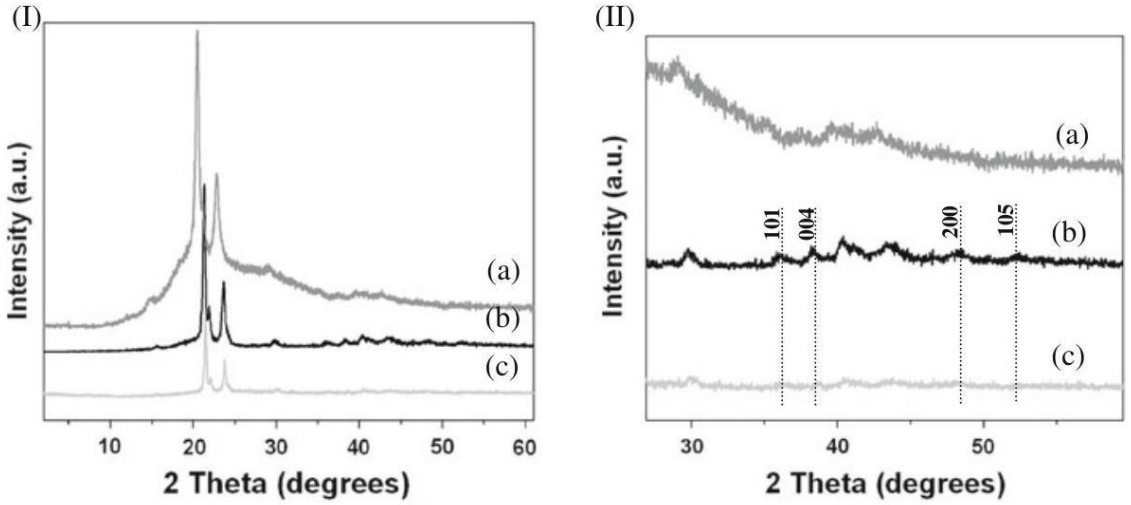

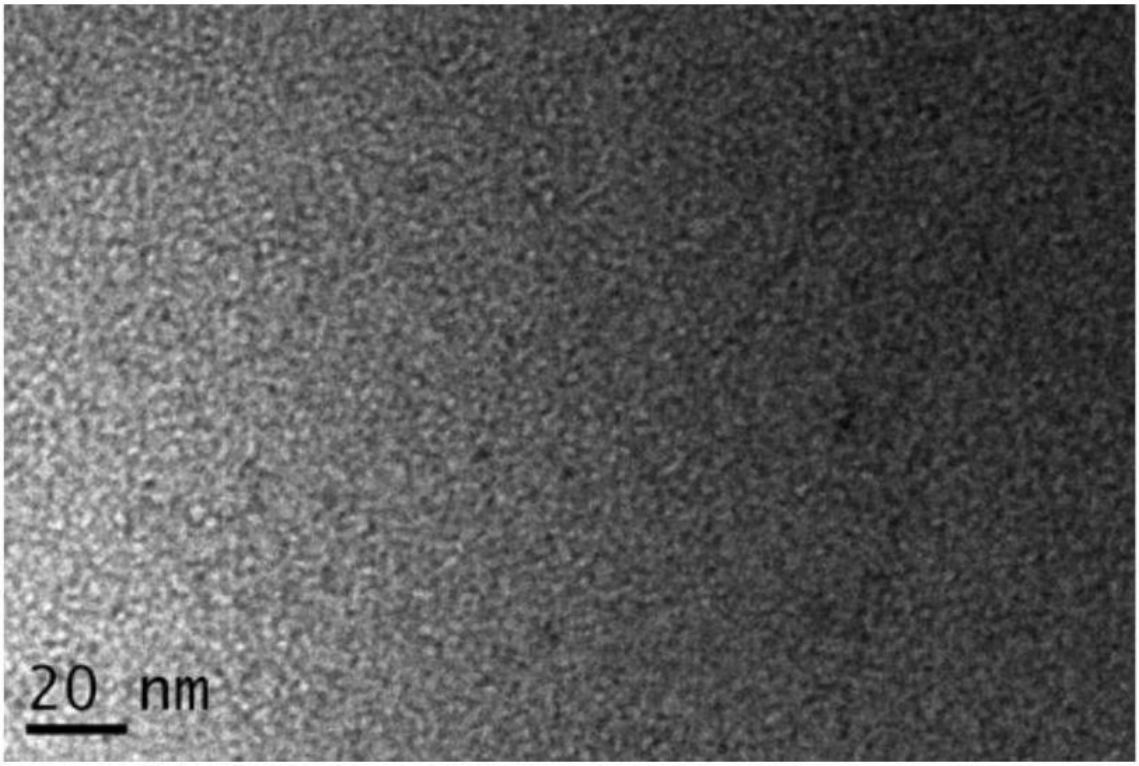

Fig. 5 TEM micrographs of PCL/TBT-5

Effect of precursor amount

Since the synthesis with acid allowed to obtain films with higher amount of titanium oxide, this method was used to investigate the effect of precursor amount. Therefore, nanocomposites with different TBT amounts (1, 5, 10 and 50wt%) were synthesized using the same HCl/TBT ratio in chloroform.

Figure 5 shows, as an example, a TEM micrograph of PCL/TBT-5 hybrid nanocomposite. A very fine morphology with well-dispersed nanoparticles can be observed. Energy-dispersive X-ray analysis of the surface pits identified Ti.

The samples containing 10 and 50wt% of TBT were analysed by XPS. BE of the C 1s, O 1s and Ti 2p and their percentage of the surface atomic contents, obtained by the area of the relevant bands in the high resolution spectra detected by XPS are summarised in Table 2.

The results of Table 2 indicate that the sample with higher amount of TBT, PCL/TBT-50, leads to an increase of TiO_2 species, which can be observed by the increase of the oxygen atoms in oxide species percentage (22.5%), indicating the higher amount of octahedral coordinated Ti^{4+} (65.9 %). Since the nanocomposite with 10wt% of TBT presents only 2.2% of TiO_2 species, the other Ti species probably interact with the polymer chain. Therefore, 10wt% seems to be the maximum amount of precursor that should be used.

Figure 6 depicts the FTIR spectra of PCL and PCL nanocomposites prepared with different amounts of TBT. The spectra of PCL and nanocomposites are dominated by strong polymer bands: two sharp bands at 2945 and 2866 cm^{-1} attributed to the $C-H$ symmetric stretching vibration of hydrocarbon of PCL, a strong band around 1730 cm^{-1} associated with carbonyl group of ester and the bands in the region of $1040-1500$ cm^{-1} due to the vibration of $C-H, C-C$ and $C-O$ of PCL [7]. Spectroscopic bands observed in the range of $3100-3700$ cm^{-1} are associated to the stretching vibration of the hydroxyl groups ($Ti-OH$) of the hybrid materials, which increase as the precursor amount increases. These hydroxyl groups that exist at the surface of titanium oxide networks due to the incomplete polycondensation have potential to form hydrogen-bonding interactions with the carbonyl groups of PCL chains.

Table 3 summarises the DSC results of PCL and the prepared nanocomposites. While the melting temperature is similar for PCL and nanocomposites with low amount, an increase is observed for the sample prepared with 50wt% of TBT. This increase can be related to the presence of higher amount of titanium oxide species in nanocomposite in agreement of XRD and XPS results, which increase the interaction between the matrix and inorganic particles.

The crystallinity of the nanocomposites decreased as the amount of inorganic phase increased, which is in agreement with literature [7, 9]. This result could be related to the formation of covalent bonds between the inorganic phase and the polymer matrix. This fact is more pronounced in the presence of lower amount of TBT. The increase in the number of bonding enhances the degree of crosslinking, making the matrix organic-inorganic more disordered, i.e. the polymer loses some of its initial crystallinity becoming more amorphous.

Young modulus of PCL and nanocomposites with different amount of inorganic phase are depicted in Fig. 7. The modulus increases as the amount of TBT increases until 5wt% of

TBT was used and then decreases slightly for higher amount of precursor. This can be explained by the interactions between the organic and inorganic phases, which increases as the amount of precursor increases. After a certain amount of TBT, agglomeration may occur and has a negative effect on modulus.

Table 2 Data of the XPS spectra in the C 1s, O 1s and Ti 2 p bands of the samples

	Ti 2p (eV) (%)		C 1s (eV) (%)			O 1s (eV) (%)		
	3/2	1/2	(C – C, C – H)	(C-O)	(C = O)	(O_2-oxide)	(C-O)	(O = C – O)
PCL	-	-	285.00	286.13	288.65	-	533.74	532.08
PCL/TBT-10	458.84 (59.0)	464.16 (41.0)	285.00 (67.7)	286.47 (18.6)	289.01 (13.6)	530.60 (2.2)	532.19 (52.6)	533.51 (45.2)
PCL/TBT-50	458.66 (65.9)	464.41 (34.1)	285.00 (73.8)	286.49 (17.5)	289.01 (8.7)	530.21 (22.5)	532.14 (54.2)	533.57 (23.3)

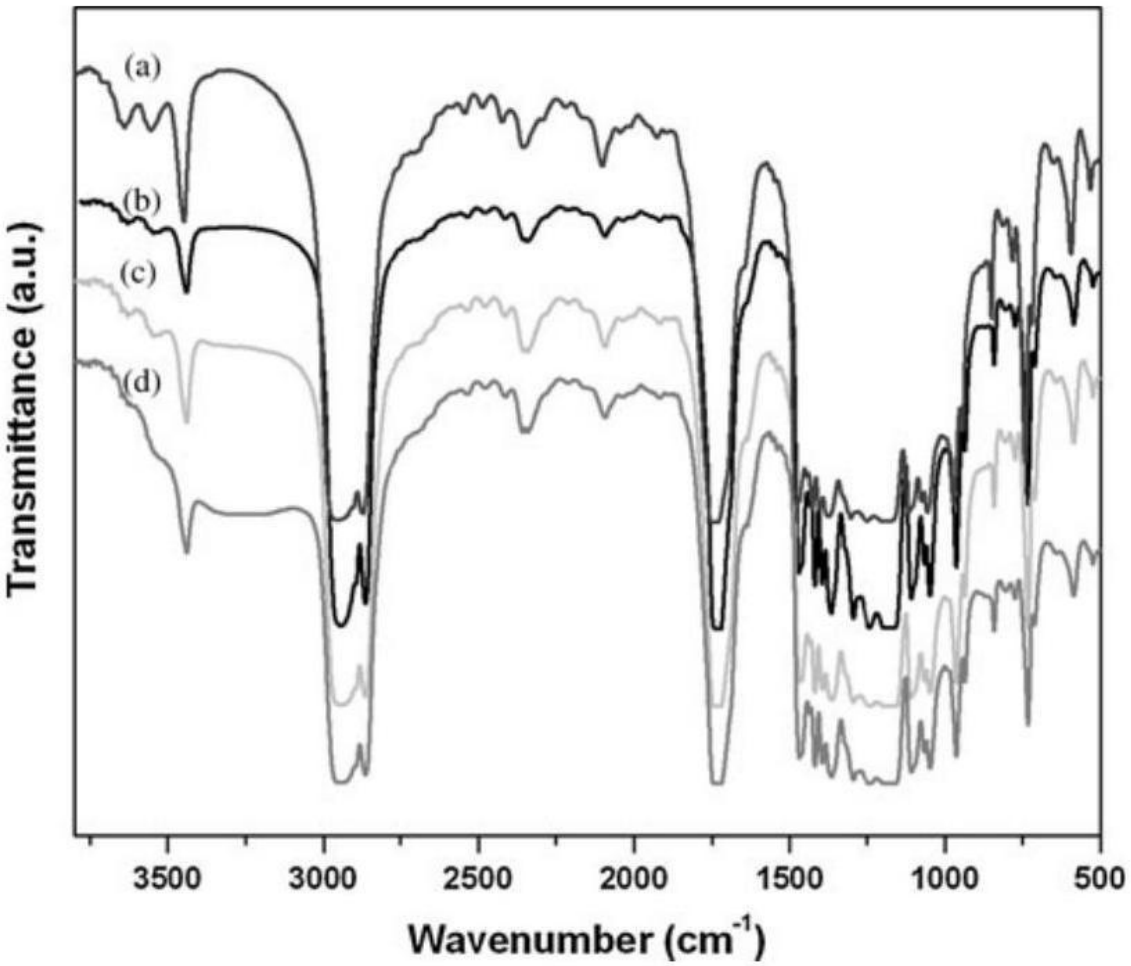

Fig. 6 FTIR spectra of the (a) PCL, (b) PCL/TBT-1, (c) PCL/TBT-5 and (d) PCL/TBT-10

Table 3 Melting temperature and crystallinity of PCL and nanocomposites

Samples	T_m(°C)	ΔH_f(J/g)	Crystallinity (%)
PCL	58.5	44.1	31.6
PCL/TBT-1	58.6	48.0	34.4
PCL/TBT-10	57.5	35.3	25.3
PCL/TBT-50	63.4	29.7	21.3

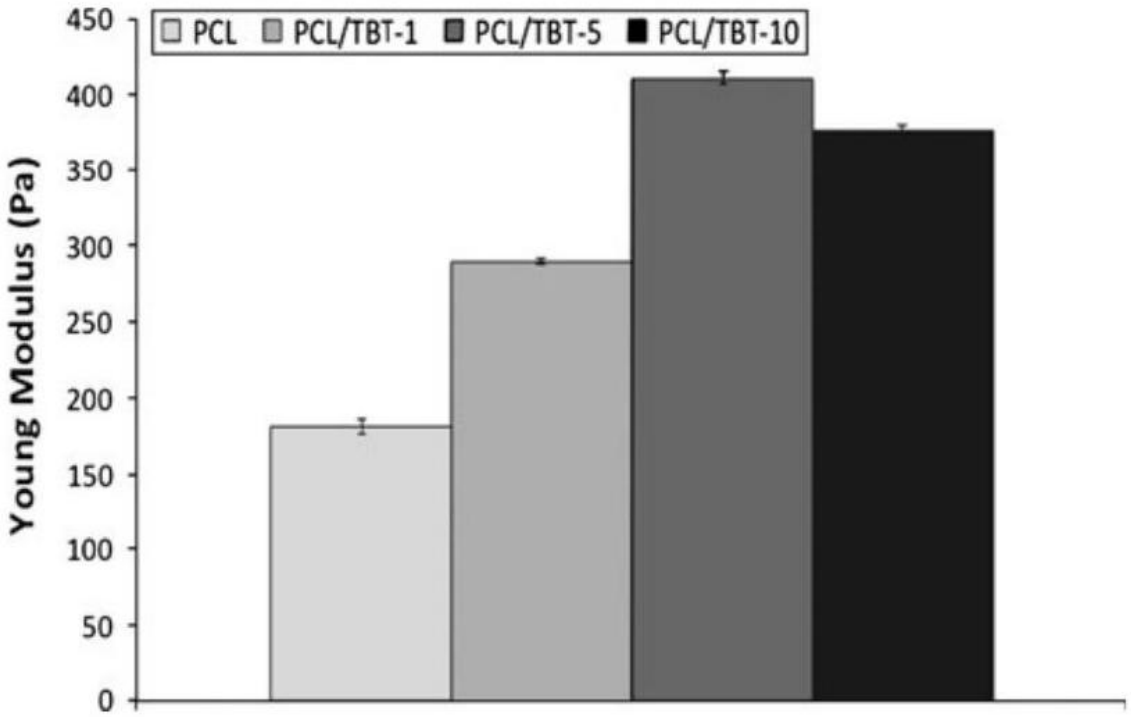

Fig. 7 Young modulus of PCL and nanocomposites

Since PCL/TBT-10 exhibited better mechanical performance, biodegradability tests were carried for this nanocomposite and PCL according to the BOD method in a closed respirometer (ISO 14851:1999). The results obtained during 40 days of biodegradation (Fig. 8) demonstrate that the nanocomposite exhibits higher biodegradability than PCL. This can be associated with the lower crystallinity of the nanocomposites as detected by DSC analysis. Since

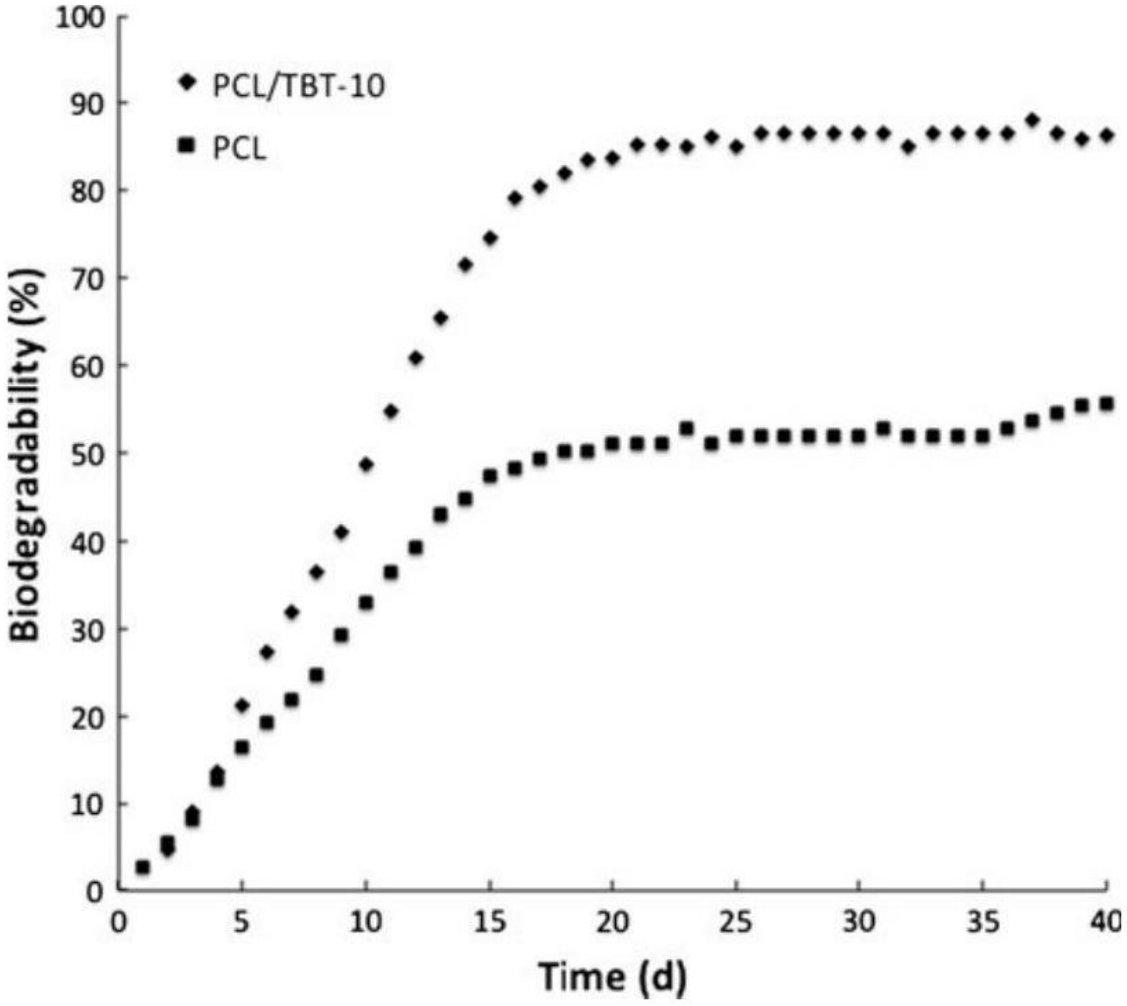

Fig. 8 Biodegradability of (a) PCL and (b) PCL/TBT-10 biodegradability takes place in the amorphous region, the increase of this region enhances this property [23].

Conclusions

Syntheses of organic-inorganic hybrid nanocomposites based on PCL using TBT, as inorganic precursor, were performed under different acid concentrations and precursor amount.

A reaction mechanism based on FTIR and NMR results was proposed using methyl acetate as model compound.

Acidic conditions favoured the reaction between TBT and PCL. The organic-inorganic hybrid nanocomposite with 10 % of TBT show the best mechanical properties and its biodegradability was higher than PCL.

Acknowledgements The authors acknowledge the financial support given by FCT through the project PTDC/AMB/73854/2006.

References

1. Wu CS (2004) J Appl Polym Sci 92: 1749
2. Liao HT, Wu CS (2004) J Polym Sci B 42:4272
3. Siuzdak DA, Start PR, Mauritz KA (2000) J Appl Polym Sci 77:2832
4. Judeinstein P, Sanchez C (1996) J Mater Chem 6:511
5. Catauro M, Raucci MG, Marco D, Ambrosio L (2006) J Biomed Mater Res B 2(77A):340
6. Boettcher SW, Bartl MH, Hu JG, Stucky GD (2005) J Am Chem Soc 127:9721
7. Li R, Nie K, Shen X, Wang S (2007) Mater Lett 61: 1368
8. Brinker CJ, Scherer GW (1990) Sol-gel science: the physics and chemistry of sol-gel processing. Academic Press Limited, New York, p 42
9. Mazzocchetti L, Scandola M, Pollicino A (2008) Polymer 49: 5215
10. Moura I, Machado AV, Duarte FM, Nogueira R (2011) J Appl Polym Sci 119:3338
11. Barlier V, Legaré VB, Boiteux G, Davenas J, Leonard D (2008) Appl Surf Sci 254:5408
12. Piszczek P, Grodzicki A, Richert M, Wojtczak A (2004) Inorg Chim Acta 357:2769
13. Caruso RA, Antonietti M, Giersig M, Hentze H-P (2001) Chem Mater 13:1114
14. Perrin FX, Nguyen V, Vernet JL (2003) J Sol-Gel Sci Technol 28:205
15. Lahav M, Kharitonov AB, Willner I (2001) Chem Eur J 7:3992
16. Zhang Z, Zuo F, Feng P (2010) J Mater Chem 20:2206
17. Chiang PC, Whang W (2003) Polymer 44:2249
18. Georgiev DG, Baird RD, Newaz G, Auner G, Witte R, Herfurth H (2004) Appl Surf Sci 236:71
19. Liaw WC, Chen KP (2007) Eur Polym J 43:2265
20. Tang X, Li Y, Chen J, Xu Y, Shen W (2007) Microporous Mesoporous Mater 103:250
21. Casaletto MP, Lisi L, Mattogno G, Patrono P, Ruoppolo G (2004) Appl Catal A 267:157
22. Moulder JF, Stickle WF, Sobol PE, Bomben KD (1995) In: Chastain J, King RC Jr (eds) Handbook of X-ray photoelectron spectroscopy. Eden Prairie, New York
23. Arillo MA, López ML, Pico C, Veiga ML, Jiménez-López A, Rodríguez-Castellón E (2001) J Alloy Compd 317-318:160